

Modeling of Erosion and Deposition of ITER Limiters During Ramp Phases

A. Kirschner¹, D. Borodin¹, V. Philipps¹, U. Samm¹, A. Loarte² and G. Federici³

¹Institut für Energieforschung – Plasmaphysik, Forschungszentrum Jülich, Association EURATOM-FZJ, Trilateral Euregio Cluster, 52425 Jülich, Germany

²ITER JWS Cadarache, St Paul-lez-Durance, France

³Fusion for Energy, Barcelona, Spain

(Received: 1 September 2008 / Accepted: 9 December 2008)

Erosion and deposition of the beryllium limiter during the ramp phases in ITER has been analyzed with the impurity transport code ERO. Physical sputtering of the beryllium limiters during the limiter phase of ramping leads to a net-erosion rate in the maximum of about 30 nm per ramping. Thus, lifetime issues seem to be uncritical from the view point of sputtering only (no material loss due to melting and other effects considered). The amount of beryllium atoms escaping into the plasma, i.e. sputtered particles, which are not redeposited, is estimated to about $3.2 \cdot 10^{21}$ per ramping, which is about 2% of the incoming deuterium ions during this time period.

Keywords: Erosion, Deposition, ITER, Beryllium Limiter, Lifetime, Impurity Transport Modelling, ERO Code.

1. Introduction

The interaction of the plasma with the wall in the limiter phase during ramp-up and -down phases of ITER has to be controlled. An acceptable lifetime of the affected wall elements as well as a low contamination of the plasma due to eroded wall material has to be ensured. One option is the use of two start-up beryllium limiters at the low field side (toroidal distance of 180°) to handle power and particle fluxes during the ramp phases.

This contribution studies the erosion and redeposition of such beryllium limiters during the ramp phases to estimate the lifetime and also the possible influx of eroded beryllium into the plasma. The erosion/deposition modeling is carried out by applying the 3D Monte-Carlo impurity transport code ERO [1] taking into account various time points of the ramp phase.

2. Modeling approach

For the ERO modeling a simplified geometry of the start-up limiters is used. Instead of the shaped limiter surface a plane limiter is assumed with a height of 2200 mm and a length in toroidal direction of 1600 mm. The magnetic field structure and plasma parameter, which is a necessary input of ERO, is provided by the ITER IT. Figure 1. shows a poloidal cross section of ITER including the shape of the last closed flux surface (LCFS) for various time points of the ramp-phase according to the temporal evolution of the plasma current I_p . The location of one of the Be limiters at the low field side of the machine is indicated in figure 1. The flux surfaces, shown

in figure 1., correspond to simulations of the ITER start-up sequence of the so-called scenario 2 (inductive operation II: 400 MW, $Q = 10$) [2].

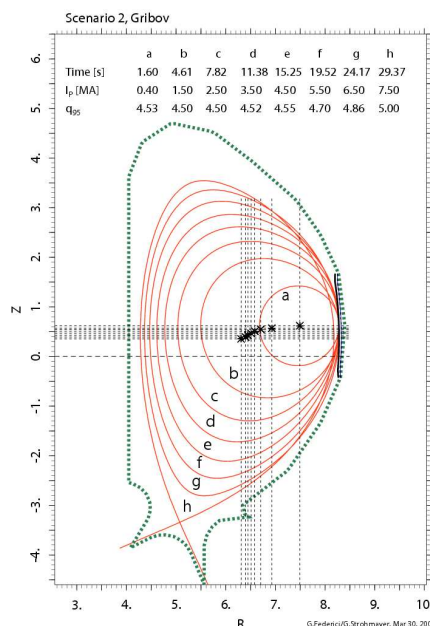


Fig. 1. Time evolution of the plasma boundary in ITER during current ramp-up (by Gribov).

The plasma for the ERO simulations is defined by the electron, ion temperature and electron density at the LCFS, i.e. $T_e(\text{LCFS})$, $T_i(\text{LCFS})$ and $n_e(\text{LCFS})$. These plasma parameters are assumed to decay exponentially perpendicular to the LCFS with decay lengths λ_{Te} , λ_{Ti} ,

author's e-mail: a.kirschner@fz-juelich.de

and λ_{ne} . In toroidal direction no variation of the plasma parameters is considered. The surface of the beryllium limiter is divided into cells of 5 mm in Z-direction and 1600 mm in toroidal direction (i.e. 440 cells in Z- and only 1 cell in toroidal direction). To study the spatial distribution of redeposited beryllium on the limiter in toroidal direction, simulations with 5 cells of 200 mm width have been carried out in addition. In general, the possible deposition of eroded beryllium outside the limiter surface is taken into account. The ERO simulation volume is taken as 2200 mm (Z) \times 40000 mm (y, toroidal) \times 300 mm (R). The toroidal length of the simulation is chosen to be large enough to avoid significant particle losses in this direction.

The incoming deuterium flux is calculated according to $\Gamma_{in} = v_{||} n_e$ with n_e the electron density along the limiter. The parallel (relative to the magnetic field) flow velocity $v_{||}$ is assumed to be constant inside the scrape-off-layer (SOL) and set to sound speed c_s . The effective flux along the limiter is then reduced corresponding to the incident angle α_B of the magnetic field. The magnetic field tends to be more and more shallow when approaching the middle part of the limiter where the LCFS touches the limiter surface. However, the flux reduction due to shallow impact (factor $\sin(\alpha_B)$) becomes questionable at shallow magnetic field lines with α_B smaller than several degrees [3]. It is well known, that even the extreme case of parallel magnetic field lines to the surface with $\sin(\alpha_B) = 0$ does not lead to zero particle flux to the surface. This is due to a combination of gyration effects, cross-field transport and sheath effects. Therefore, two different assumptions are analyzed in this work: a constant angle of α_B along the whole target according to the largest B-field angle and thus representing an upper limit for the particle flux along the limiter surface and a reduction factor according to geometrical impact angle, which results in reduced fluxes representing a lower limit.

3. Modeling results

3.1. Ramp-up at plasma current $I_p = 4.5$ MA

At plasma current of $I_p = 4.5$ MA, corresponding to time point $t = 15.25$ s in the ramping phase, the plasma boundary has the configuration (e) as shown in figure 1. Within scenario 2 this corresponds to plasma temperature and density at the LCFS of $T_e(\text{LCFS}) = T_i(\text{LCFS}) = 50$ eV and $n_e(\text{LCFS}) = 1.71 \cdot 10^{12}$ cm $^{-3}$. The decay for temperature and density is assumed to be exponential, perpendicular to the LCFS with decay lengths of $\lambda_{Te} = 7.5$ cm, $\lambda_{Ti} = 15$ cm and $\lambda_{ne} = 5$ cm.

3.1.1 Constant magnetic field along limiter surface

Outside the LCFS (inside the SOL) a parallel flow velocity of $v_{||} = c_s$ is assumed. Inside the LCFS $v_{||}$ is set to

$0.5 \cdot c_s$. The influence of zero flow velocity inside the LCFS is analyzed later. Sticking of sputtered Be particles returning to the limiter surface is calculated using TRIM [4] reflection coefficients. For comparison a sticking factor of unity is assumed. The cross-field diffusion coefficient for impurities is assumed to be 0.2 m 2 /s.

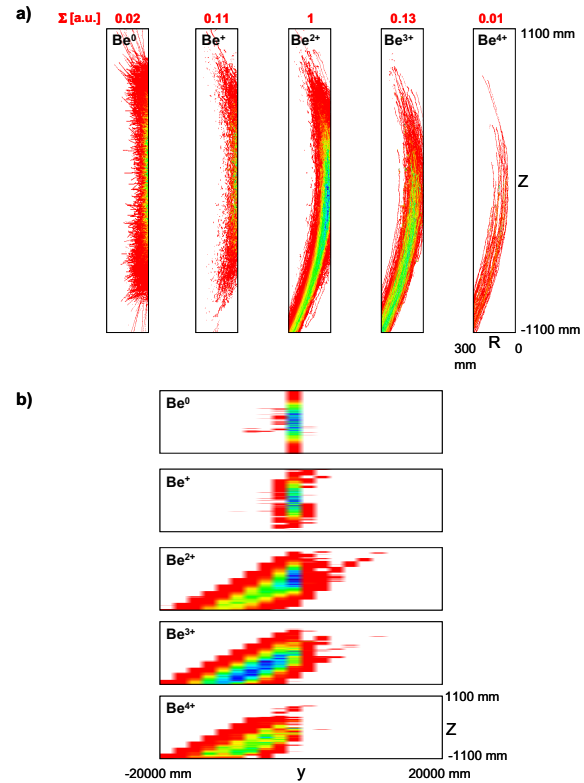


Fig. 2. Modeled density of beryllium atoms and ions above limiter surface. **a)** Integrated in toroidal direction y; **b)** Integrated in R-direction. The numbers in red represent the integrated particle densities of the different charge states, normalized to the maximum.

Figure 2a. shows the modeled distributions of Be atom and ion densities in the plasma above the limiter integrated over the toroidal direction and figure 2b. shows the same data but integrated over the R direction. The transport of beryllium ions along the magnetic field lines is clearly seen, which leads to a loss of eroded Be particles into the minus Z direction.

The fraction of lost particles in the various directions relative to the number of sputtered atoms is summarized in table 1. As already concluded from figures 2a. and 2b., main loss (more than 40%) takes place in minus Z direction. However, also a significant number of particles (about 20%) leave the simulation volume in R direction. This also can be seen from figure 2a at negative Z positions.

	Particle losses (relative to sputtered)
Z_{min}	43%
Z_{max}	0.04%
y_{min}	0%
y_{max}	0.2%
R	22%

Table 1. Modeled particle losses.

The amount of particles lost in the other directions can be neglected. All particles, which are not lost out of the simulation volume, are redeposited. The amount of Be redeposition on the limiter itself can be accounted to about 16% relative to the number of sputtered particles.

Figure 3. shows profiles of gross-erosion, redeposition and net-erosion along the limiter surface. Redeposition occurs naturally outside the Be limiter surface in toroidal direction (compare bottom part of figure 3.). Here, the amount of redeposition is about 18%. On the limiter, the Be net-erosion in the maximum is about $1.2 \cdot 10^{20}/\text{m}^2\text{s}$ corresponding to a net-erosion rate of about 1.2 nm/s, with an atomic density of $0.123 \text{ atoms}/\text{\AA}^3$ for Be. As can be seen from figure 3., beryllium net-erosion does not differ significantly from the gross-erosion. This results from the relatively low amount of redeposition. The self-sputtering due to eroded Be particles returning to the limiter surface is not included in the calculations shown in figure 3., but has been calculated and leads to an increase of the erosion by about 5% only.

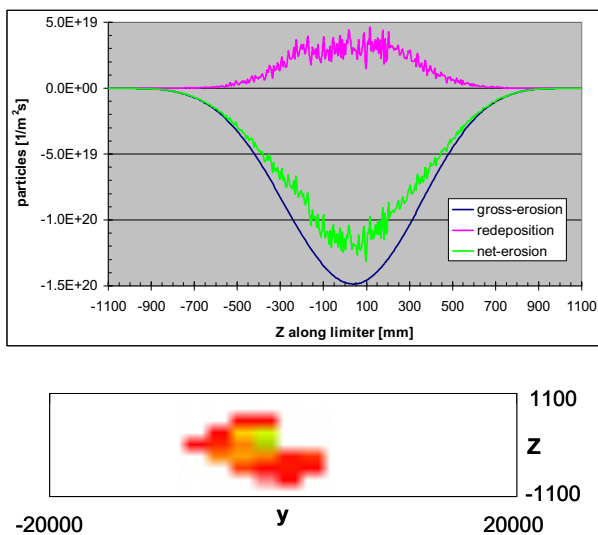


Fig. 3. Profiles of gross-erosion, redeposition and net-erosion along the limiter surface, integrated in y -direction (top). Two dimensional distribution of the redeposition (bottom).

3.1.2 Varying magnetic field impact angle at the limiter surface

So far a constant magnetic field angle of $\alpha_B = 2.2^\circ$ along the limiter surface has been used to calculate the impinging deuterium flux to the surface. Using instead the geometrical impact angle, the deuterium flux along the surface and accordingly the erosion decreases as shown in figure 4. On the limiter surface the amount of Be redeposition relative to the amount of sputtered particles is unchanged ($\sim 20\%$). The overall redeposition including the area outside the limiter increases from 34% to about 41%. The absolute amount of erosion is reduced especially in the middle part of the limiter where the

magnetic field is nearly parallel to the limiter surface. This is also the region near to the LCFS, where the loss of eroded particles is maximal: magnetic field lines inside the LCFS are closed and do not strike the surface again – eroded particles penetrating deeply into this region have a low probability to return to the surface. Thus, the maximum net-erosion at the limiter decreases by a factor of about 4 compared to the case of a constant field angle of 2.2° .

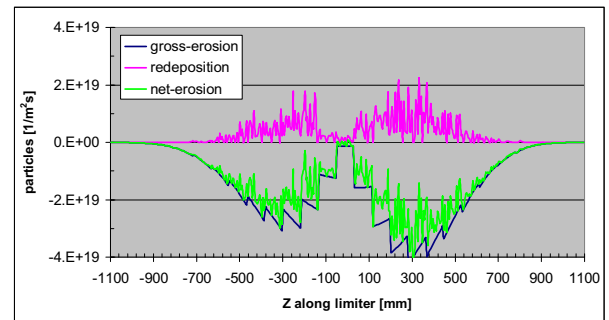


Fig. 4. Profiles of gross-erosion, redeposition and net-erosion along the limiter surface using varying magnetic field angle along the limiter surface.

3.1.3 Influence of parallel flow velocity inside the last closed flux surface

If the parallel flow velocity inside the LCFS is assumed to be zero, the overall amount of redeposition (including the area outside the limiter surface) increases to about 55%. Using instead a directed flow in this region, the ionized particles are thermalized and move parallel to the B field. With the given B field direction this assumption leads to an increased loss of particles along the B field in the minus Z direction. In the case of zero flow velocity inside the LCFS the direction of the particle movement is randomly – about one half of the particles gyrates along the B-field backwards to the limiter and the other half away from the limiter. Therefore significantly more particles can return to the surface, which increases the redeposition probability.

3.1.4 Influence of sticking assumption for Be atoms

The extreme assumption of a sticking factor of unity for the Be atoms returning to the surfaces does not significantly increase the deposition efficiency compared with the case using TRIM reflection. Using the TRIM-like reflection, the redeposition pattern is more expanded in toroidal direction. However, the simulation volume in this direction has been chosen to be large enough such that no significant losses appear in this direction. Therefore, the absolute amount of redeposition does not significantly depend on the sticking assumptions.

3.2 Additional ramp-up time points

In addition to the simulations at $t = 15.25$ s (4.5 MA) two further time points of the ramping phase have been used: $t = 7.82$ s (2.5 MA) and $t = 24.17$ s (6.5 MA) corresponding to plasma boundaries marked as “c” and “g” in figure 1. The electron and ion temperature at the LCFS are assumed to be unchanged compared to the 4.5 MA case (i.e. 50 eV and 150 eV, respectively) and also the same decay lengths have been used. The electron density at the LCFS is set to $1.12 \cdot 10^{12}$ cm⁻³ and $2.15 \cdot 10^{12}$ cm⁻³ for the 2.5 MA and 6.5 MA case. Again, the same decay lengths as for the 4.5 MA case have been assumed. Other simulation parameters (in particular parallel flow velocity, cross field diffusion coefficient, reflection coefficient of returning beryllium particles) are set to values as discussed in 3.1.1. The magnetic field angle along the surface (defining the incoming deuterium ion flux) is kept constant choosing the largest value for both cases – 1.8° for 2.5 MA and 2.5° for 6.5 MA – this represents an upper limit of the incoming flux and thus the gross-erosion, as discussed above.

The modeled profiles of gross-erosion, redeposition and net-erosion are shown in figure 5., for the cases of 2.5 and 6.5 MA. The maximum gross-erosion is about a factor of 2 larger for the 6.5 MA case than for 2.5 MA. This is due to the higher electron density but also due to the less shallow magnetic field angle along the surface. The erosion profile is spatially more extended in the 6.5 MA case, which is a result of a larger “curvature radius” of the plasma boundary (see figure 1.).

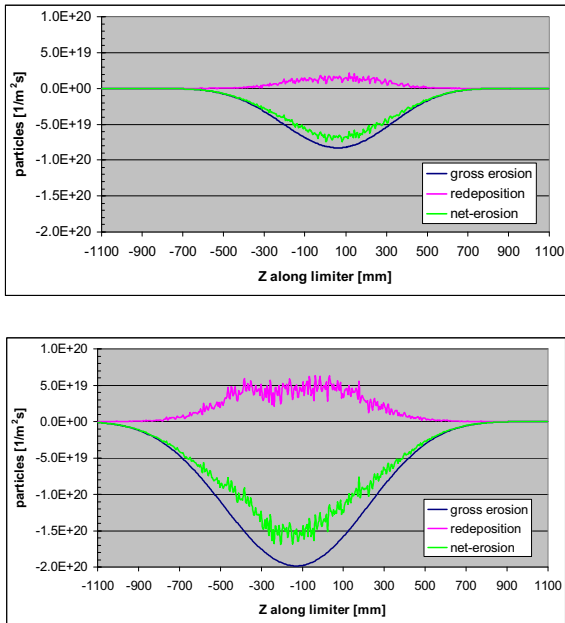


Fig. 5. Profiles of gross-erosion, redeposition and net-erosion along the limiter surface for plasma current of 2.5MA (top) and 6.5MA (bottom).

Table 2. summarizes the integrated gross-erosion on the limiter surface, the maximum gross- and net-erosion and the (integrated over the surface) amounts of redeposition on the limiter itself and outside the limiter surface. The corresponding values for the 4.5 MA case are also included.

	2.5MA	4.5MA	6.5MA
Integrated gross-erosion on limiter [particles/s]	$8.6 \cdot 10^{19}$	$1.8 \cdot 10^{20}$	$2.8 \cdot 10^{20}$
Maximum gross-erosion [particles/m²s]	$8.3 \cdot 10^{19}$	$1.5 \cdot 10^{20}$	$2.0 \cdot 10^{20}$
Maximum net-erosion [particles/m²s]	$6.9 \cdot 10^{19}$	$1.2 \cdot 10^{20}$	$1.6 \cdot 10^{20}$
Redeposition on limiter	13%	16%	19%
Redeposition outside limiter	17%	18%	15%

Table 2. Integrated gross-erosion, gross- and net-erosion in the maximum and amounts of redeposition (relative to gross-erosion, integrated over the surface) for different time points (or plasma currents) of the ramp phase.

As for the 4.5 MA case the main particle loss occurs in minus Z direction also for 2.5 and 6.5 MA. To estimate the overall particle loss (i.e. the amount of beryllium particles escaping into the main plasma) and maximum net-erosion of the beryllium limiter (determining its life time) during the ramp phases, the data of the three ramp-up cases are integrated over the following time intervals:

at 2.5 MA: 4.61 s to 11.54 s (duration: 6.93 s)
at 4.5 MA: 11.54 s to 19.71 s (duration: 8.17 s)
at 6.5 MA: 19.71 s to 29.37 s (duration: 9.66 s)

The configuration at 2.5 MA is extended to the time point of the 1.5 MA configuration according to figure 1., and the 6.5 MA configuration is extended to the end of the limiter phase. With a limiter size of $2.2 \times 1.6 = 3.5$ m² and using the values from table 2., a total Be net-erosion results as:

$$(8.6 \cdot 10^{19} - 30\%) \cdot 6.93 \text{ s} + (1.8 \cdot 10^{20} - 34\%) \cdot 8.17 \text{ s} + (2.8 \cdot 10^{20} - 34\%) \cdot 9.66 \text{ s} = 3.2 \cdot 10^{21} \text{ beryllium particles,}$$

which escape into the plasma during ramping. In this calculation about 56% of these particles originate from the 6.5 MA, 31% from the 4.5 MA and 13% from the 2.5 MA configuration. The number of escaping beryllium particles can be compared with the number of $1.5 \cdot 10^{23}$ deuterium ions impinging the limiter surface during ramping (using the same weighting over the time).

To estimate the lifetime of the beryllium limiters the maximum net-erosion rates from table 2. are taken with the same weighting over the time. The maximum net-erosion of the different cases (2.5 MA, 4.5 MA and 6.5 MA) does not occur at the same location on the limiter wherefore the following estimation represents an upper limit. The calculation leads to an erosion rate of $3 \cdot 10^{21}$ beryllium atoms per m^2 and ramp phase. With an atomic beryllium density of $0.123 \text{ atoms}/\text{\AA}^3$, a net-erosion rate of 30 nm per ramping is obtained. Assuming a thickness of the beryllium armor layer of 4 mm this would result in a lifetime of about 130.000 rampings or 65.000 discharges with two rampings (up and down) per discharge.

4. Conclusions

Physical sputtering of the beryllium limiters during the limiter phases of ramping in ITER leads to a modeled net-erosion rate in the maximum of about 30 nm per ramping. Thus, lifetime issues seem to be uncritical from the view point of sputtering only (no material loss due to melting and other effects are considered here). The amount of beryllium atoms escaping into the plasma, i.e. sputtered particles, which are not redeposited is estimated to about $3.2 \cdot 10^{21}$ per ramping, which is about 2% of the incoming deuterium ions during this time period.

The presented simulations do not take into account sputtering due to impurities. However, there could be a certain influx of e.g. oxygen and beryllium and depending on the ITER wall material choice also carbon and tungsten. With an electron temperature of 50 eV the beryllium sputter yield due to these impurities is up to a factor of about 10 larger than the sputtering due to D or T. A rough estimation of the effective sputtering assuming 10% impurities in the edge plasma with a 10 times larger sputter yield compared to D on Be leads to two times larger gross erosion of beryllium. This still would result in a lifetime of about 32.000 discharges.

Within the parameter variations presented in this work the amount of redeposited beryllium on the limiter was not larger than 20% relative to the amount of gross erosion. Depending on the assumptions for the parallel flow velocity inside the scrape-off-layer this number even could be smaller. However, in any case the amount of redeposition already is relatively small and thus the overall simulation results just can be affected in the extreme case (without any redeposition) by about 20%.

It might be worth to note that experiments at the linear plasma simulator PISCES have shown an enhanced erosion of Be at elevated surface temperatures [5]. It is seen that at surface temperatures above about 900K the Be erosion is larger than expected from physical sputtering. This is presently explained in terms of adatom evaporation with the condition that adatom sublimation dominates over adatom recombination. However, the

plasma conditions discussed for the ITER ramp phase here lead to estimated surface temperatures clearly below 900K even at the location of maximum power load.

The study of the influence of the heat load deposited on the beryllium limiters is out of the scope of this paper. In [6] a detailed assessment of the power load on the start-up limiters is presented. It is concluded that at high plasma current the power load is close to the engineering limit and it is suggested that the limiter shape has to be optimized.

The present ITER design is changing, which may lead to abandon the concept of dedicated Be movable start up limiters as implied in this work. Instead, the main chamber wall may act as start up area but with a “shaped” structure to avoid leading edges. In a continuation of this work the erosion and redeposition behavior of such a wall design can be analyzed similar as described here.

Acknowledgments

This work has been carried out under EFDA 06-1388 and the European Task Force for Plasma-Wall Interaction.

References

- [1] A. Kirschner *et al.*, Nucl. Fus. **40**, No. 5, 989 (2000).
- [2] G. Federici *et al.*, “Simulations of ITER start-up for limiter power load assessment”, ITER D 2229DE v1.2.
- [3] D. Tskhakaya and S. Kuhn, J. Nucl. Mat. **313-316**, 1119 (2003).
- [4] W. Möller and W. Eckstein, Comput. Phys. Commun. **51**, 355 (1988).
- [5] R.P. Doerner *et al.*, J. Nucl. Mat. **337-339**, 877 (2005).
- [6] M. Kobayashi *et al.*, Nucl. Fus. **47**, 61 (2007).